Energy 44 (2012) 702–709

Contents lists available at SciVerse ScienceDirect

Energy

journal homepage: www.elsevier.com/locate/energy

Study on the thermal behavior of different date palm residues: Characterization and devolatilization kinetics under inert and oxidative atmospheres

Yassine El may [a,b], Mejdi Jeguirim [a,*], Sophie Dorge [a], Gwenaelle Trouvé [a], Rachid Said [b]

[a] Laboratoire Gestion des Risques, Environnement 3 bis rue Alfred Werner, 68093 Mulhouse, France[1]
[b] Unité de Recherche d'Etude des Milieux Ionisés et Réactifs (UR EMIR), IPEIM, Avenue Ibn El Jazzar Monastir 5019, Tunisia[2]

ARTICLE INFO

Article history:
Received 6 March 2012
Received in revised form
4 May 2012
Accepted 11 May 2012
Available online 9 June 2012

Keywords:
Date palm residues
Pyrolysis
Oxidation
Devolatilization
Thermogravimetry
Kinetic parameters

ABSTRACT

Date palm residues are an attractive source of biomass energy since they are renewable, abundantly available and do not compete with food crops. Pyrolysis and combustion may be efficient methods of exploiting energy from these biomass resources. The purpose of this research was to investigate the thermal behavior of date palm biomass in order to evaluate their usefulness for energy production. In fact, ultimate and proximate analyses as well as thermal behavior of different date palm residues (date palm leaflets (DPL), date palm rachis (DPR), date palm trunk (DPT), date stones (DS) and fruitstalk prunings (FP)) were investigated. Non-isothermal thermogravimetric analyses (TGA) were performed to assess fuel reactivities under inert and oxidative atmospheres. Thermal degradation of all samples has exhibited quite similar behavior except DS. In contrast, different properties (e.g., reactivity, HHV or activation energy) were obtained, which may be attributed to a difference between tree parts composition (branches, trunk, fruit…). Thus, DPT and FP were found to be the most reactive materials in inert conditions; while in oxidative conditions, DPR is the highest one. In addition, activation energies corresponding to devolatilization regions under inert and oxidative conditions were 49.8, 45.2, 52.7, 50.9, 89.1 kJ mol^{-1} and 58.9, 49.6, 67.6, 57.7, 110.7 kJ mol^{-1} for DPL, DPR, DPT, DS and FP respectively. The obtained data, sample properties along with thermal behavior under inert and oxidative atmospheres as well as kinetic parameters, allowed the comparison of the obtained results with other biofuels and can be useful for the design of processing system for energy productions.

© 2012 Elsevier Ltd. All rights reserved.

1. Introduction

Utilization of agricultural residues as an energy resource has received in the last decades much attention. In fact, these biomasses have various economical and environmental advantages [1]. It is may be a promising solution which does not interfere with the production of food and contribute to cover energy needs.

Tunisia, like the developing countries, needs to identify and to exploit all their available resources in the context of national sustainable development. Significant reserves of renewable energy forms are not yet used in this country. Solar energy and biomass can be among the major sources of energy production for the next years. Main sources of biomass include agriculture waste, such as olive and date palm wastes. Although the energetic valorization of olive waste has received considerable attention [2–8], few investigations on the characterization and thermal behavior of date palm residues are found in literature [9,10].

The date palm (*Phoenix dactylifera*) is one of the most cultivated palms in the arid and semi-arid regions of the world. The tree stem is unbranched and is covered by old remaining leaves or palms (Fig. 1). It is characterized by numerous offshoots that are produced at the base of the trunk of young palms. The date palm may reach an age of over 100 years and average mature tree is about 20 m tall. New palms appear as a crown at the top of the stem. The two parts of palm are rachis which is the main axis and series of leaflets on each side of a common petiole. On a dry weight basis, in the whole palm the amount of leaflets is (46%) and rachis is (53.4%) [11]. An adult date palm tree has approximately 100–125 green palms with an annual formation of 10–26 new leaves [12]. It is estimated that the number of date palms worldwide is about 105 million [13]. The world production of dates has registered considerable expansion over the last decade. Indeed, the production has moved from 6,542,760 tons in 2004–7,429,811 tons in 2009 [14].

Tunisia has approximately 4.5 million trees, covering an area of 32,000 ha [15]. Tunisia is currently among the top 10 world

---

* Corresponding author. Tel.: +33 3 89336166; fax: +33 3 89336161.
E-mail address: mejdi.jeguirim@uha.fr (M. Jeguirim).

[1] Tel.: +33 3 89336166; fax: +33 3 89336161.

[2] Tel.: +216 73 500 273; fax: +216 73 500 512.

0360-5442/$ – see front matter © 2012 Elsevier Ltd. All rights reserved.
doi:10.1016/j.energy.2012.05.022

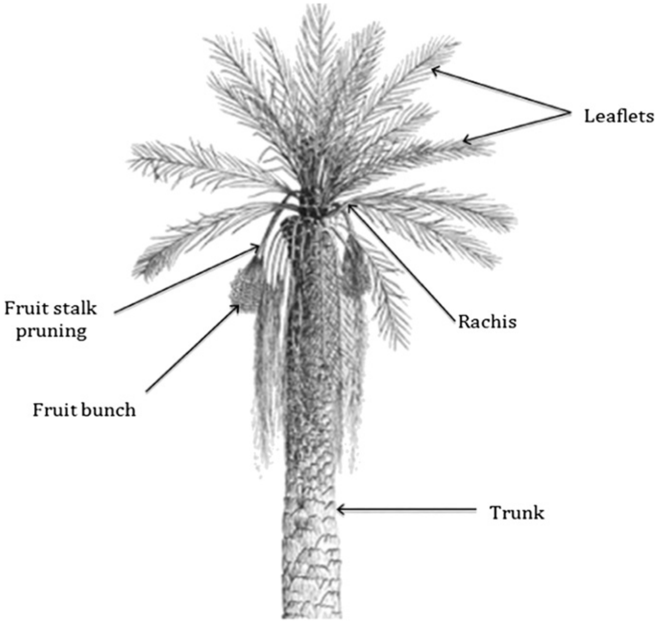

Fig. 1. Date palm tree.

producer and the first exporter of dates in value. During the last years, Tunisian production has reached an average of 145,000 tons per year. In spite of the fruits that are worldwide consumed, these trees generate important quantities of agricultural residues and agro-industrial by-products. In fact, during date fruit harvesting important quantities of date palm by-products such as leaves, fruitstalk prunings, fruit wastes and date stones are generated. In addition, trunk becomes available upon natural or accidental death of the palm or by forced removal when plantations oasis are renewed. For example, the date stones represent about 10% of the date produced weight [16]. Therefore, an average of 22 leaves per date palm per year produces approximately more than 198,000 tons per year of leaves in Tunisia [17]. Hence, these wastes are abundantly available and a valorization method seems to be necessary.

Different date palm residues are traditionally used in many sectors [17,18]. Among these uses, date palm residues and particularly leaves are used for preparing pulp and paper. They are also sources for reinforcing fibers for polymeric matrices in composite materials [19,20]. Date stones are, also, used as biosorbent [21] and for preparing activated carbons by physical or chemical activation [22]. Recently, experimental work was conducted to study some physical properties of date palm wood. The obtained results showed that this material can be efficiently used in the manufacturing of buildings for thermal insulation [11]. Nevertheless, few published studies evaluating the potential use of date palm by-products as a renewable energy source were found in literature. In particular, Al Omari has examined the potential of date stones and palm stalks as an energy source. This study investigates the conversion of both date palm residues to thermal energy via combustion at different experimental conditions in a small scale furnace with a conical solid fuel bed. The author has noted that these biomasses are technically a viable alternative in the heat generation installations [9].

In a later paper, the same author compared the combustion and heat transfer characteristics obtained in a furnace using date stones as a fuel, with those found in the case of coal. It seems that date stones contain much volatile compounds leading under sufficiently high amounts of combustion air to a higher combustion and heat transfer rates per unit mass of the fuel compared to the tested coal [10].

The aim of this work is to study for the first time the thermal behavior of different date palm residues (date palm leaflets (DPL), date palm rachis (DPR), date palm trunk (DPT), fruitstalk prunings (FP), and date stones (DS)) via thermogravimetric analysis. Reports and data about the thermal behavior and kinetics of date palm wastes are not available in literature. The first part of this study is devoted to the determination of the physico-chemical characteristics. TGA studies are carried out in both inert and oxidative atmospheres. Finally, thermal degradation characteristics as well as kinetics parameters are evaluated for the selected samples.

2. Experimental

2.1. Materials

Five biomass samples used in this study were obtained from a date palm oasis in Tozeur, Tunisia. They were cut into small pieces (for DPL) and/or grounded (for DPT, DPR, DS and FP) in order to have homogenous products. These different residues were naturally dried in the sun during 2–3 days in order to reduce water content. After sieving, the samples with particle size between 1 and 2 mm were collected for the experimental tests.

2.2. Chemical analysis

In order to obtain the properties of the biomass materials related to the thermo-chemical conversions, proximate and ultimate analyses were performed. Ultimate analysis corresponding to the elemental compositions of the samples was performed by Service Central d'Analyses (Vernaison, France).

Proximate analysis was carried out using a thermogravimetric analyzer (CAHN 121 thermobalance) with gas flowing upward through the furnace at 12 NL/h. The proximate TG method involves heating the samples (under N_2) at a rate of 10 °C min^{-1}, from room temperature to 110 °C with a hold up time of 10 min to obtain the weight loss associated with moisture. Temperature is then ramped at 20 °C min^{-1}–900 °C with a hold up of 10 min to obtain the weight loss associated with volatiles release. Oxygen is then introduced into the furnace chamber to oxidize char formed and the weight loss associated with this step is the fixed carbon. The remaining material after oxidation is the ash. At the start of each experiment, 30 min of N_2 purging was conducted.

Besides, the heating values were measured using a REKA adiabatic oxygen bomb calorimeter.

2.3. Thermogravimetric analyses

Thermogravimetric analyses have been widely used to study the thermal degradation characteristics of agricultural wastes and other materials [23–35]. In this study, the thermal behavior of the biomass materials was studied under inert and oxidative atmospheres using a CAHN 121 thermobalance. TGA experiments were performed at heating rates of 5 °C min^{-1} (gas flow of 12 NL/h) from room temperature to 900 °C. Slow heating rate was selected to allow studying the thermal behavior under conditions where the transport processes do not hide the study of the chemistry effects [24]. Experimental tests were carried out in both inert and oxidative atmospheres to investigate different steps of thermal degradation of each biomass material and to determine reaction kinetic parameters.

3. Results and discussion

3.1. Date palm residues characterization

Proximate and ultimate analyses along with bulk densities were carried out to characterize the different date palm wastes. The obtained results are given in Table 1. The analysis findings show that tested samples have high content of volatiles, carbon, hydrogen and oxygen. On the contrary, the relative contents of nitrogen and sulfur are low. In comparison with biomass, these materials have typical composition [25]. Heating values (LHV) were at intervals raging from 15.2 to 19.0 MJ kg^{-1}. These values are in the same order of magnitude as the results obtained for sawdust, olive solid waste, oil palm fruit bunches, Miscanthus, wood pellets and wood chips (Table 1). Comparison with literature data for wood biomass and energetic crops shows that the investigated biomasses have typical composition [24,25,28,29]. Among date palm residues, date stones (DS), which have the highest percentage of volatiles (VM) and fixed carbon (FC) and the lowest ash content, present the highest calorific values in term of low heating value (LHV). Large differences are observed for amounts of humidity and ash and may explain variation of the LHV values.

Important characteristic of biomass materials is their bulk density which is in relation to transport and storage costs. The value of this property for DS is very high (656 kg m^{-3}), which overtakes the one of wood chips (550 kg m^{-3}). Both heating value and bulk density define the energetic density (ED) that is the potential of energy available per volume of biomass. Values of ED show the same trend as the values of bulk density. DS close to the one of wood pellets (12 GJ m^{-3}) is much higher than the remained samples. It is worth noting that DS is the most attractive material for energy production due to its high energetic density and then low cost transportation. However, it is necessary to examine the thermal degradation behavior in order to select the most convenient date palm residue.

3.2. Thermal behavior under inert atmosphere

The thermal degradation characteristics of the samples under inert atmosphere at a heating rate of 5 °C min^{-1} are shown in Fig. 2. Despite, the differences between samples in evolution profiles of mass loss (TGA) and the time derivative of the mass loss (DTG), the pyrolysis curves of DPW follow the usual shape of lignocellulosic materials [23]. Indeed, the five samples demonstrate four regimes of weight loss in the TGA and DTG analyses: moisture loss, hemicellulose decomposition, cellulose decomposition and a last step corresponding to the lignin decomposition which is distributed along a wide temperature interval [25]. The first mass loss region due to moisture release and light volatiles loss occurs between 25 °C and 150 °C. The apparently higher release from DPR and DPT could be due to simultaneous moisture and low temperature volatiles release. Then, devolatilization, which is the main pyrolysis of samples, starts at proximately 180, 160, 165, 170 and 190 °C for DPL, DPR, DPT, DS and FP respectively. Such variations in initial degradation temperatures of biomass have been related to the differences in the elemental and chemical compositions of the samples [38]. The major weight loss (where the main degradations occurred) ended at approximately 367, 333, 327, 334 and 372 °C for the same sample sequence. During this step, two decomposition processes corresponding to the degradation of hemicellulose and cellulose are observed. For the pyrolysis of DPL, DPR, DPT and FP, there are two distinct regions of DTG curves. The first region appears as a more or less pronounced shoulder at approximately 238, 210, 220 and 261 °C for DPL, DPR, DPT and FP. However, the following second region is characterized by peaks with maxima at 315, 287, 297 and 308 °C for the four samples respectively. Appearance of shoulders could be generated by the decomposition of hemicellulose and some of the lignin. However, the obtained peak should correspond to the decomposition of cellulose and the remaining of lignin. When hemicellulose and cellulose decompositions overlap, the shoulder marks the peak of the hemicellulose decomposition [24]. In contrast with the previous four samples, DS has only one maximum rate of decomposition observed at about 257 °C followed by two small shoulders located at the higher temperature side on the DTG curve. The maximum peak of DTG curve is may be attributed to an overlapping between hemicellulose and cellulose decomposition steps and the small shoulders can be associated to the decomposition of the cellulose and lignin. At the end of this decomposition step, a continuous slight devolatilization is observed, which can be attributed to the slow degradation of lignin. Table 2 summarizes TG curves characteristics in terms of pyrolysis temperature ranges as well as temperatures of DTG shoulders and peaks.

Rate of mass loss as indicated by the DTG is an indication of the material reactivity. Hence, it is observed that the rate of decomposition of the light component (hemicellulose) in the case of DS is greater than the rate of decomposition of the heavy component (cellulose). Rate of the heavy component decomposition is dominated for DPL, DPR, DPT and FP. The maximum rates of weight loss (% s^{-1}) ranged from 0.040 to 0.096 for the samples (Table 2). These values are higher compared to other biomasses tested by Jeguirim and Trouvé [29] as well as Grønli et al. [24] in the same

Table 1
Proximate and ultimate analysis and bulk density of DPW.

Biomass samples	References	Proximate analysis (%), wet basis				LHV[a]	BD	ED	Ultimate analysis (%), wet basis				
		Moisture	VM	FC	Ash				C	H	O	N	S
DPL	This work	7.1	68.0	9.7	15.2	19.0	312	5.9	40.8	6.0	35.2	0.63	0.21
DPR	This work	12.1	73.6	8.3	6.0	15.2	173	2.6	39.8	5.7	43.0	0.19	0.26
DPT	This work	10.0	71.8	11.5	4.2	15.5	213	3.3	42.76	5.8	45.5	0.21	0.12
DS	This work	6.4	74.1	17.5	1.2	17.4	656	11.4	51.2	6.4	40.9	0.73	<0.20
PF	This work	9.8	66.8	16.8	2.8	15.2	140	2.1	42.7	5.8	40.9	<0.30	<0.20
Sawdust	[7]	1.3	63.1	23	12.6	18.0	–	–	46.5	5.96	–	<0.30	–
OSW	[27]	7.4	66.6	23.8	2.16	19.8	–	–	57.6	8.08	27.7	1.34	0.17
EFP	[32]	7.95	83.9	10.78	5.36	18.7			49.1	6.48	38.3	0.7	<0.10
Miscanthus	[34]	10.0	78.8	09.5	02.7	16.7	–	–	43.7	05.7	44.8	01.1	0.2
Wood pellets	[36]	7.14	–	–	0.65	17.4	693	12.0	49.80	6.3	43.5	0.40	0.01
Wood chips	[37]	34.9	51.6	13.3	0.2	11.7	550	6.43	47.3	6.1	46.0	<0.10	0.40

VM: volatile matter, FC: fixed carbon, LHV: low heating values (MJ kg^{-1}), BD: bulk density (kg m^{-3}), ED: energetic density (GJ m^{-3}), DPL: date palm leaflets, DPR: date palm rachis, DPT: date palm trunk, DS: date stones, PF: fruitstalk prunings, OSW: olive solid waste, EFP: oil palm empty fruit bunches.

[a] Calculated based on dry free ash.

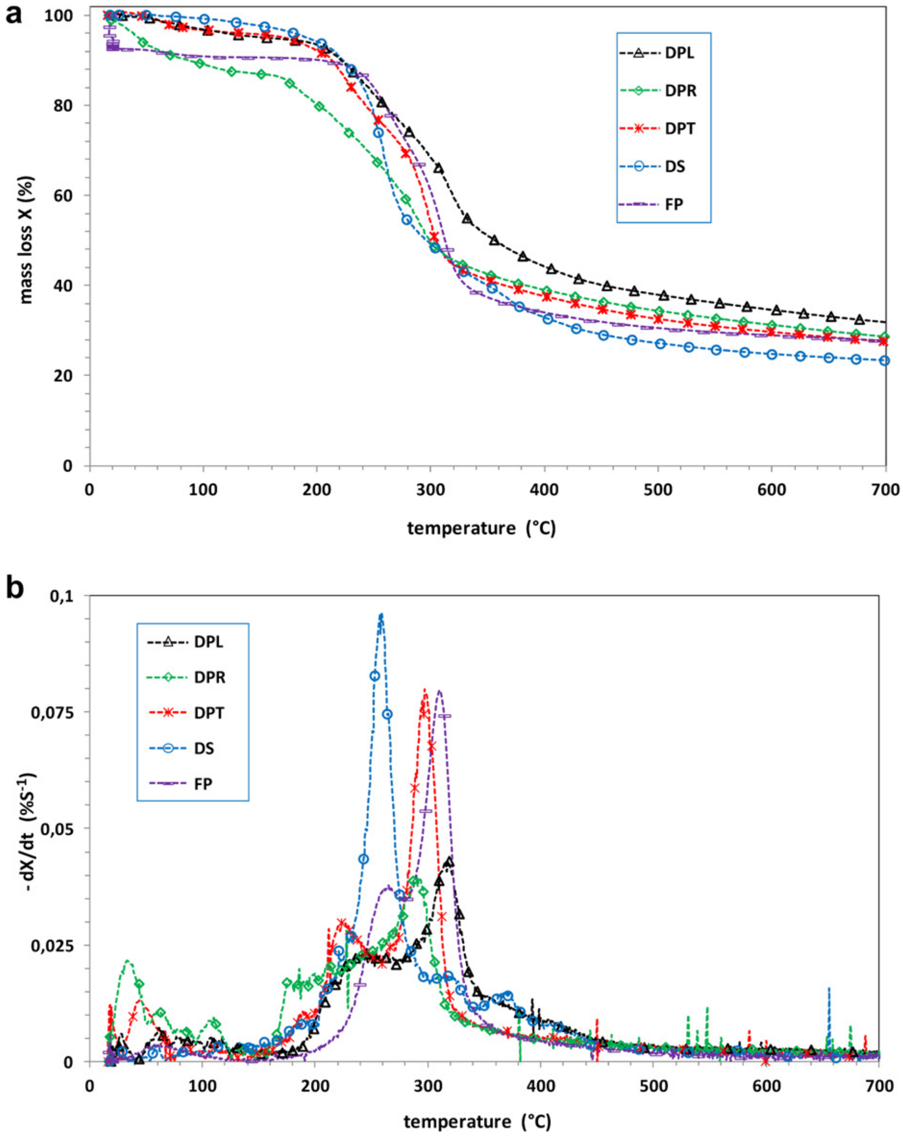

Fig. 2. TGA (a) and DTG (b) curves during the pyrolysis of samples under inert atmosphere.

experimental conditions. However, they are quite similar to the ones obtained for olive oil mill wastewater and sawdust samples [7].

On the other hand, Table 2 also shows the reactivity R_M, which is directly proportional to the maximum weight loss R_{DTGmax} and inversely proportional to the value of its corresponding temperature T_{DTGmax}. Calculation of samples reactivity is based on the method proposed in previous investigations [26,30,39]:

$$R_M = 100 \sum \frac{R_{\mathrm{DTG\ max}}}{T_{\mathrm{DTG\ max}}} \quad (1)$$

where, R_M the reactivity (% s^{-1} $^{\circ}\mathrm{C}^{-1}$), R_{DTGmax} is the maximum weight loss rate (% s^{-1}) and T_{DTGmax} the corresponding peak temperature (°C).

Reactivity (R_M) is equal to 0.23 and 0.24% s^{-1} $^{\circ}\mathrm{C}^{-1}$ for DPL and DPR, while it is higher for DPT, DS and PF, around

Table 2
Characteristics of the thermogravimetric experiment under inert atmosphere.

Sample	Temperature range for pyrolysis (°C)	R_{shoulder} (% s^{-1})	T_{shoulder} (°C)	R_{peak} (% s^{-1})	T_{peak} (°C)	$R_M \times 10^3$ (% s^{-1} $^{\circ}\mathrm{C}^{-1}$)	Residue (%) (900 °C)
DPL	178–500	0.023	243	0.043	315	0.23	28.4
DPR	155–605	0.021	211	0.040	290	0.24	23.1
DPT	177–586	0.030	223	0.080	297	0.40	24.2
DS	170–482	–	–	0.096	258	0.37	21.6
PF	209–543	0.038	265	0.080	309	0.40	25.0

R_{shoulder}: rate shoulder (% s^{-1}); T_{shoulder}: temperature shoulder (°C); R_{peak}: rate peak (% s^{-1}); T_{peak}: temperature peak (°C); R_M: reactivity (% s^{-1} $^{\circ}\mathrm{C}^{-1}$).

0.37–0.40% s^{-1} $^{\circ}C^{-1}$. DPT and FP reactivity are the highest ones followed by DS and DPR, respectively. These values are similar to the ones obtained by Munir et al. during pyrolysis of four different agricultural residues (ranged between 0.31 and 0.54% s^{-1} $^{\circ}C^{-1}$) [26].

3.3. Thermal behavior under oxidative atmosphere

TGA and DTG of the five samples (DPL, DPR, DPT, DS and FP) under oxidative atmosphere at a heating rate of 5 °C/min are plotted versus temperature in Fig. 3. It is seen that weight losses present three main steps: the first accounts for moisture evaporation, the second is due to devolatilization and the last relates to the oxidation of char. The first stage under oxidizing atmosphere ranges from room temperature to approximately 125 °C. Loss of water and volatilization of light molecules may have contributed to weight loss in this stage. The second stage of weight loss occurs at temperatures between 141 °C and 347 °C (Table 3), depending on the waste. It is noted that the four maximum of decomposition rates occur at about 305, 265, 298, 261 and 265 °C for DPL, DPR, DPT, DS and FP, respectively. At the end of oxidation, residual mass of DPL is about 14.5% of the initial mass which is higher than the ash obtained for DPR (7.1%), DPT (2.6%), DS (0.9%) and for FP (11.3%). It should be noted that a fuel with a higher percentage of ash in its composition, presents a lower initial temperature of degradation [38]. These effects justify the results from proximate analysis and explain the DTG behavior. In addition, for samples combustion with high ash contents, consideration must be given to incorporate an efficient ash removal from installation. As evidence from DTG curves in Fig. 3(b) and (a) close similarity is shown for all the wastes during char oxidation phase, expect DS. Char oxidation from DS needs high temperature to proceed. Compared to the four other wastes, DS char oxidation peak is shifted toward higher temperatures. It occurs in the temperature range of 421 °C and 509 °C for DS while this region proceeds between 366 °C and 447 °C for the other samples. On the other hand, the reactivity values (R_M) for oxidation (Table 3) show that DPR is the most reactive materials followed by DPT, FP, DPL and DS respectively.

Characteristic combustion parameters such as initial ignition and burnout temperature and corresponding times, as well as maximum rate of mass loss derived from the TG and DTG curves can be used to assess relative burning properties of samples (Table 4). Temperatures are defined as follows: ignition temperature (T_i) which is defined according to Xiang-guo et al. [40] and

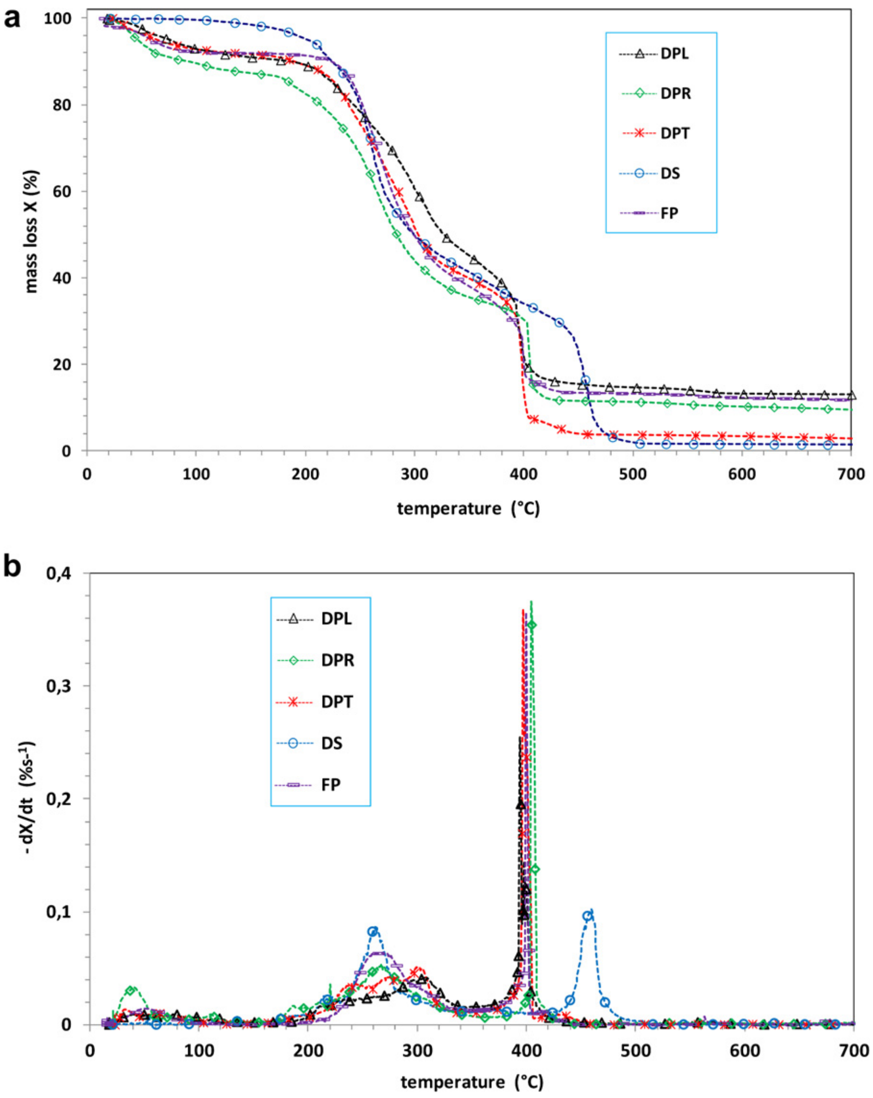

Fig. 3. TGA (a) and DTG (b) curves during the oxidation of samples under oxidative atmosphere.

Table 3
Characteristics of the thermogravimetric experiment under oxidative atmosphere.

Sample	Devolatilization zone			Char combustion zone			$R_M \times 10^3$ (% s^{-1} °C^{-1})	Ash (%) (900 °C)
	Temperature range	R_{peak} (% s^{-1})	T_{peak} (°C)	Temperature range	R_{peak} (% s^{-1})	T_{peak} (°C)		
DPL	170–337	0.041	305	366–439	0.249	394	0.76	12.50
DPR	167–347	0.051	265	382–425	0.373	404	1.11	08.03
DPT	170–331	0.050	298	366–447	0.367	397	1.09	01.74
DS	141–336	0.086	261	421–509	0.103	459	0.55	01.20
PF	200–333	0.063	265	371–436	0.357	499	0.96	11.20

R_{peak}: maximum rate (% s^{-1}); T_{peak}: temperature peak correspond to maximum rate (°C); R_M: reactivity (% s^{-1} °C^{-1}).

burnout temperature (T_b) where DTG profile reaches a 1% per minute combustion rate.

As can be seen (Table 4), DS sample with high volatile content presents the lowest ignition temperature, while ignition temperature of FP is the highest one. This behavior is in agreement with the results obtained by Vamvuka and Safakiotakis during the investigation of biomass and coal degradation under oxidative atmosphere [41]. Moreover, high burnout temperature is exhibited by DS (474 °C), while the fibrous samples show relatively lowest burnout temperature ranged between 403 and 413 °C. This point was previously observed by Khalfi et al. Authors demonstrated that due to their lower conductive heat transfer, fibrous materials having lower bulk density ignited and reacted more rapidly than samples having higher bulk density [42].

To further investigate combustion behavior of the samples, an ignition index (D) and a combustion index (S) are proposed according the two following equations [41]:

$$D = \frac{R_{\max}}{(t_{\max} t_i)} \tag{2}$$

$$S = \frac{R_{\max} R_a}{\left(T_i^2 T_b\right)} \tag{3}$$

where $R_{\max}$ is the maximum combustion rate, $t_{\max}$ and t_i are times correspond to maximum combustion rate and ignition temperature, respectively. R_a is the average mass loss rate under oxidative atmosphere.

A comparison between sample values of the two mentioned characteristic indexes is shown in Table 4. Ignition performance of samples increases with the increase of ignition index value D. Also, the better combustion reactivity can be assigned to the high value of combustion index S. Therefore, it can be concluded that samples which burn at lower temperature and shorter time, are the most reactive materials. Thereby, DPT can be considered to be the most reactive material, followed by DPR, DPL and FP, whereas DS is the less reactive material.

Table 4
Characteristic combustion parameters of samples.

sample	T_i (°C)	t_i (s)	R_a (10^{-2} % s^{-1})	$R_{\max}$ (% s^{-1})	$t_{\max}$ (s)	T_b (°C)	t_b (s)	$D \times 10^7$	$S \times 10^{10}$
DPL	221	2530	0.820	0.249	4630	410	2530	0.21	1.02
DPR	222	2490	0.866	0.373	4700	413	2490	0.32	1.59
DPT	222	2480	0.921	0.367	4600	406	2480	0.32	1.69
DS	210	2340	0.941	0.103	5380	474	2340	0.08	0.46
FP	232	3160	0.817	0.357	6370	403	3160	0.18	1.34

T_i: ignition temperature (°C); t_i: time correspond to ignition temperature (s); R_a: average mass loss rate under oxidative atmosphere; $R_{\max}$: maximum combustion rate; $t_{\max}$: time correspond to maximum combustion rate (s); T_b: burnout temperature (°C); t_b: time correspond to burnout temperature (s); D: ignition index; S: combustion index.

3.4. Kinetic analysis

Thermal analysis techniques have been used in the estimation of kinetics parameters of biomass and other combustible material [36]. Several approaches of the kinetic analysis of non-isothermal TGA data have been used for the determination of the kinetic parameters for biomass thermal degradation. The kinetic analysis of dynamic results aims to relate the experimentally values of conversion rate of sample mass against temperature with values predicted for models. In the present paper, study of kinetic schemes for both devolatilization regions under inert and oxidative atmospheres is based on the Arrhenius equation [43].

The rate equation used in all kinetics studies can be written as:

$$\frac{dx}{dt} = kx^n \tag{4}$$

where x is the conversion ratio, which is defined as $x = (m_0 - m)/(m_0 - m_f)$ (m is the mass at any time and subscripts 0 and f respectively refer to the initial and final masses at the end of that stage). K and n are the reaction constant and the reaction order, respectively. Applying the Arrhenius equation (5), the combined equations (4) and (5) lead to a linear form equation (6) as:

$$k = A \exp\left(-\frac{E}{RT}\right) \tag{5}$$

$$\ln\left[\frac{-1}{m_0 - m_f}\frac{dm}{dt}\right] = \ln(A) - \left(\frac{E}{RT}\right) + n \ln\left(\frac{m - m_f}{m_0 - m_f}\right) \tag{6}$$

where dm/dt is the ratio of mass change with time, A is the pre-exponential factor and R is the universal gas constant (gas value). Equation (7) may be written under the linear form:

$$y = B + Cx + D^*Z \tag{7}$$

where

$$y = \ln\left[-1/m_0 - m_f \, dm/dt\right],\ x = 1/T,$$
$$z = \ln\left(m - m_f/m_0 - m_f\right),\ B = \ln(A),\ C = -E/R,\ D = n$$

Constants B, C, D are estimated by multi-linear regression of the TGA data for each stage using Microsoft Excel. The kinetic parameter results (pre-exponential factor, activation energy and reaction order) and the coefficients of determination, R^2, for each experiment are reported in Table 5. These data cannot be supported by literature since the current study is unique. However, it is important to compare the obtained results with the other ones from literature.

Pyrolysis of FP has the highest value of activation energy (89.1 kJ mol^{-1}), while all the other samples have close values ranged between 45.2 and 52.7 kJ mol^{-1}. The same experimental and analytical procedure applied by Dorge et al. to Miscanthus

Table 5
Kinetic parameters during devolatilization step under inert and oxidative atmosphere.

Biomass sample	Pyrolysis					Oxidation				
	Temperature range (°C)	E (kJ mol^{-1})	ln A (s^{-1})	n	R^2	Temperature range (°C)	E (kJ mol^{-1})	ln A (s^{-1})	n	R^2
DPL	170–346	49.8	2.4	0.52	92	160–350	58.9	6.2	0.76	95
DPR	138–333	45.2	3.5	0.68	90	138–331	49.6	4.5	0.73	89
DPT	136–322	52.7	4.9	0.46	96	135–340	67.6	8.4	0.84	97
DS	134–333	50.9	4.7	0.71	91	146–350	57.7	6.3	0.92	90
FP	162–367	89.1	12.7	1.04	96	180–335	110.7	18.3	1.15	95
Cotton stalk[a]	–	77.0	–	0.5	98	–	113	–	0.5	99
Shea meal[a]	–	67.0	–	0.5	81	–	108	–	0.5	82
Sawdust[b]	–	41.7	2.8	0.5	97.6	–	107.8	17.4	1	95
Corn stover[c,d]	–	57.95	9.5	0.74	91	–	57.32	9.9	0.75	81

E: apparent activation energy (kJ mol^{-1}); A: pre-exponential factor (s^{-1}); n: order of reaction; R^2: Regression coefficient.

[a] [26].

[b] [7].

[c] [44].

[d] Under heating rate of 10 °C min^{-1}.

pellets pyrolysis yielded low values of both E (89 kJ mol^{-1}) and A (ln $A = 13$ s^{-1}) [35]. FP has also a high value of pre-exponential factor (Ln $A = 12.7$ s^{-1}) compared to the other four samples with ln A ranged from 2.4 to 4.9 s^{-1}.

For oxidation, the same behavior is noted with high values for both energy activation and pre-exponential factor ($E = 110.7$ kJ mol^{-1}, ln $A = 18.3$ s^{-1}) for FP compared to the other samples. A change in the atmosphere from nitrogen (inert) to air (oxidative) clearly results in an increase of the kinetic parameter values for DPW. This behavior is in agreement with findings of Munir et al. [26]. Reaction orders are given for the main devolatilization step for both pyrolysis and oxidation in Table 5. For pyrolysis, a reaction order of 0.46–1.04 is obtained, whereas sample values on oxidative atmosphere increase (0.76–1.15). A similar reaction order was obtained during the pyrolysis of sawdust and impregnated sawdust [7], *Arundo donax* [29] and Miscanthus straw [34].

4. Conclusions

In this work five biomass residue samples from Tunisian date palm cultivation were characterized and tested under inert and oxidative atmospheres in TGA. Ultimate and proximate analyses of samples, heating values and density bulk have allowed to obtain chemical and thermal characterizations of samples. A common approach was used for modeling kinetic parameters on the devolatilization of the different samples under the 2 atm.

The high energy density of DS makes it the most attractive material for energy recovery. In any case, the heating values of the remained materials are sufficiently attractive to overcome the problems associated with low energetic density. On the other hand, from TGA and DTG curves it was possible to determine thermal degradation behavior and to obtain information on reactivity. It was shown that despite the different fuels characteristics, the thermal degradation profiles were similar among the samples, except for DS. Among the samples studied, DPT was the most reactive material under both pyrolysis and oxidative atmosphere, whereas DS was the less reactive fuel. Activation energies associated with develotilization step in both pyrolysis and oxidation were 49.8, 45.2, 52.7, 50.9 and 89.1 kJ mol^{-1} and 58.9, 49.6, 67.6, 57.7 and 110.7 kJ mol^{-1} for DPL, DPR, DPT, DS and PF, respectively. It was checked that the change in the atmosphere from nitrogen to air increased the value of activation energy for the different DPW.

References

[1] Lee S, Speight JG, Loyalka SK. Handbook of alternative fuel technologies. CRC Press, Taylor & Francis Group; 2007.

[2] Masghouni M, Elhassayri M. Energy applications of olive-oil industry by-products: – I. The exhaust foot cake. Biomass and Bioenergy 2000;18:257–62.

[3] López MC, Blanco CG, Martimez-Alonso A, Tascou JMD. Composition of gases released during olive stones pyrolysis. Journal of Analytical and Applied Pyrolysis 2002;65:313–22.

[4] Caputo Antonio C, Scacchia F, Pelagagge PM. Disposal of by-products in olive oil industry: waste-to-energy solutions. Applied Thermal Engineering 2003;23:197–214.

[5] Garcia-Ibañez P, Sanchez M, Cabanillas A. Thermogravimetric analysis of olive-oil residue in air atmosphere. Fuel Processing Technology 2005;87:103–7.

[6] Chouchene A, Jeguirim M, Khiari B, Trouvé G, Zagrouba F. Study on the emission mechanism during devolatilization/char oxidation and direct oxidation of olive solid waste in a fixed bed reactor. Journal of Analytical and Applied Pyrolysis 2010;87:168–74.

[7] Chouchene A, Jeguirim M, Trouvé G, Favre-Reguillon A, Le Buzit G. Combined process for the treatment of olive oil mill wastewater: absorption on sawdust and combustion of the impregnated sawdust. Bioresource Technology 2010;101:6973–82.

[8] Chouchene A, Jeguirim M, Favre-Reguillon A, Trouvé G, Le Buzit G, Khiari B, et al. Energetic valorisation of olive mill wastewater impregnated on low cost absorbent: sawdust versus olive solid waste. Energy 2012;39:74–81.

[9] Al-Omari SAB. Experimental investigation on the combustion and heat transfer characteristics in a furnace with unconventional biomass fuels (date stones and palm stalks). Energy Conversion and Management 2006;47:778–90.

[10] Al-Omari SAB. Evaluation of the biomass “date stones” as a fuel in furnaces: a comparison with coal combustion. International Communications in Heat and Mass Transfer 2009;36:956–61.

[11] Bendahou A, Dfresne A, Kaddami H, Habibi Y. Isolation and structural characterization of hemicelluloses from palm of *Phoenix dactylifera L.* Carbohydrate Polymers 2007;68:601–8.

[12] Zaid A, Arias-Jimenez EJ. Date palm cultivation. In: Harris PS, editor. FAO plant production and protection paper. Rome: FAO; 2002. p. 156. Rev. 1.

[13] Agoudjil B, Benchabaneb A, Boudennec A, Ibos L, Fois M. Renewable materials to reduce building heat loss: characterization of date palm wood. Energy and Buildings 2011;43:491–7.

[14] FAOSTAT. On-line statistical database of the food and agricultural organization of the United Nations. Available online at: http://apps.fao.org; 2010.

[15] Rhouma A. Le palmier dattier en Tunisie – Le patrimoine génétique, vol. II. Rome, Italy: IPGRI; 2005.

[16] Haimour MN, Emeish S. Utilization of date stones for production of activation carbon using phosphoric acid. Waste Management 2006;26:651–60.

[17] Bchini H, Hsayoui S, Aloui S. Gestion de la matière organique et compostage des palmes sèches dans le milieu oasien. Annales de l’INRAT 2002;75:299–312.

[18] Barreveld WH. Date palm products. FAO agricultural services bulletin no 101, Rome193.

[19] El Morsy MMS. Studies on the rachis of Egyptian date palm leaves for hardboard production. Fibre Science and Technology 1980;13:317–21.

[20] Khiari R, Mhenni MF, Belgacem MN, Mauret E. Chemical composition and pulping of date palm rachis and posidonia oceanic – a comparison with other wood and non-wood fibre sources. Bioresource Technology 2010;101:775–80.

[21] Belala Z, Jeguirim M, Belhachemi M, Addoun F, Trouvé G. Biosorption of basic dye from aqueous solutions by date stones and palm-trees waste. Kinetic, Equilibrium and Thermodynamic Studies, Desalination 2011;271:80–7.

[22] Bouchelta C, Medjram MS, Bertrand O, Bellat JP. Preparation and characterization of activated carbon from date stones by physical activation with steam. Journal of Analytical and Applied Pyrolysis 2008;82:70–7.

[23] Órfão JJM, Antunes FJA, Figueiredo JL. Pyrolysis kinetics of lignocellulosic materials—three independent reactions model. Fuel 1999;78:349–58.

[24] Grønli MG, Varhegyi G, Di Blasi C. Thermogravimetric analysis and devolatilization kinetics of wood. Industrial and Engineering Chemistry Research 2002;41:4201–8.

[25] Wilson L, Weihong YW, Blasiak W, John GR, Mhilu CF. Thermal characterization of tropical biomass feedstocks. Energy Conversion and Management 2011;52:191–8.

[26] Munir S, Daood SS, Nimmo W, Cunliffe AM, Gibbs BM. Thermal analysis and devolatilization kinetics of cotton stalk, sugar cane bagasse and shea meal under nitrogen and air atmospheres. Bioresource Technology 2009;100:1413–8.

[27] Chouchene A, Jeguirim M, Khiari B, Trouvé G, Zagrouba F. Thermal degradation behavior of olive solid waste: influence of the particle size and oxygen atmosphere. Resources Conservation and Recycling 2010;54:271–7.

[28] Jeguirim M, Dorge S, Trouvé G. Thermogravimetric analysis and emission characteristics of two energy crops in air atmosphere: arundo donax and *Miscanthus giganthus*. Bioresource Technology 2010;101:788–93.

[29] Jeguirim M, Trouvé G. Pyrolysis characteristics and kinetics of arundo donax using thermogravimetric analysis. Bioresource Technology 2009;100:4026–31.

[30] Ghetti P, Ricca L, Angelini L. Thermal analysis of biomass and corresponding pyrolysis products. Fuel 1996;75:565–73.

[31] Chen WH, Po-Chih Kuo. Isothermal torrefaction kinetics of hemicellulose, cellulose, lignin and xylan using thermogravimetric analysis. Energy 2011;36:6451–60.

[32] Sulaiman F, Abdullah N. Optimum conditions for maximising pyrolysis liquids of oil palm empty fruit bunches. Energy 2011;36:2352–9.

[33] Yong HY, Sang DK, Jong ML, Keun HL. Kinetic studies of dehydration, pyrolysis and combustion of paper sludge. Energy 2002;27:457–69.

[34] Jeguirim M, Dorge S, Loth A, Trouvé G. Devolatilization kinetics of miscanthus straw from thermogravimetric analysis. International Journal of Green Energy 2010;7:164–73.

[35] Dorge S, Jeguirim M, Trouvé G. Thermal degradation of miscanthus pellets: kinetics and aerosols characterization. Waste and Biomass Valorization 2011; 2:149–55.

[36] Verma VK, Brama S, Delattin F, Laha P, Vandendael I, Hubin A, et al. Agro-pellets for domestic heating boilers: standard laboratory and real life performance. Applied Energy 2012;90:17–23.

[37] Senneca O. Kinetics of pyrolysis, combustion and gasification of three biomass fuels. Fuel Processing Technology 2007;88:87–97.

[38] Mansaray KG, Ghaly AE. Thermal degradation of rice husks in nitrogen. Bioresource Technology 1998;65:13–20.

[39] Park SW, Jang CH. Effects of pyrolysis temperature on changes in fuel characteristics of biomass char. Energy 2012;39:187–95.

[40] Xiang-guo L, Bao-guo M, Li X, Zhen-wu H, Xin-gang W. Thermogravimetric analysis of the co-combustion of the blends with high ash coal and waste tyres. Thermochimica Acta 2006;441:79–83.

[41] Vamvuka D, Sfakiotakis S. Combustion behaviour of biomass fuels and their blends with lignite. Thermochimica Acta 2011;526:192–9.

[42] Khalfi A, Trouvé G, Delfosse L, Delobel R. Influence of the apparent density during the burning of wood waste furniture. Journal of Fire Sciences 2004;22: 229–50.

[43] Brown ME. Introduction to thermal analysis techniques and applications. Kluwer Academic Publisher; 2002.

[44] Kumar A, Wang L, Dzenis YA, Jones DD, Hanna MA. Thermogravimetric characterization of corn stover as gasification and pyrolysis feedstock. Biomass and Bioenergy 2008;32:460–7.